

This submitted manuscript has been authored by a contractor of the U.S. Government under contract No. W-31-109-ENG-38. Accordingly, the U.S. Government retains a nonexclusive, royalty-free license to publish or reproduce the published form of this contribution, or allow others to do so, for U.S. Government purposes.

ANL-HEP-PR-82-04

CDF-123

CENTRAL SHOWER COUNTER PROTOTYPE FOR THE FERMILAB COLLIDER DETECTOR FACILITY*

L. Nodulman, R. Diebold, N. Hill, B. Musgrave,
J.R. Sauer, R. Wagner, and A.B. Wicklund
Argonne National Laboratory
Argonne, Illinois 60439, U.S.A.

H. Kautzky
Fermi National Accelerator Laboratory
Batavia, Illinois 60510, U.S.A

Abstract

The construction of a full scale prototype shower counter for the FNAL Collider Detector Facility central calorimetry is described in detail. Beam tests provide results on performance parameters.

*Work supported by the U.S. Department of Energy.

(submitted to Nuclear Instruments and Methods in Physics Research)

1. Introduction

The Fermilab Collider Detector Facility (CDF) will be a powerful general purpose detector system for studying antiproton proton collisions at 2 TeV using the Tevatron as a storage ring. The CDF design¹ calls for central shower counters as part of a calorimetry system of projective towers located outside a solenoid coil. The overall layout of the CDF central detectors is shown in Figure 1 and the basic geometry of one of the 48 modules of the central calorimeter system is shown in Figure 2. Each tower covers 15° of azimuth by approximately 0.1 units of pseudorapidity. A full scale prototype shower counter module of the hybrid scintillator/strip chamber design^{2,3} has been constructed and tested in the M5 test beam at Fermilab, in conjunction with a prototype central hadron calorimeter. We report here on the design, construction, and performance of this prototype shower counter.

Important considerations in the design were the cost and ease of construction, energy resolution, position resolution, electron identification, and ease of calibration and monitoring. The design resulted from a program of shower counter studies carried out in the M5 test beam at FNAL^{2,4}. Tests of a small scale prototype strip chamber have been described previously³.

2. Design and Construction

The prototype module is essentially the same as the idealized module of Figure 2 and is 98 in. long. The two ends are one inch steel plates serving as structural members⁵. At the end corresponding to a polar angle of 90°, 5/8 in. is allowed for mechanical, chamber gas, and other connections. At the other end, a 2 in. space is allowed for connections and the light guides for the last two towers. Thus the scintillator coverage is 93 3/8 in. long. There are 33 layers of scintillator, 32 layers of 1/8 in. lead, and two

multiwire proportional strip chambers at depths of 2.5 and 6 radiation lengths for normal incidence. The division of the module into 10 towers is given by polar angle segments of equal increment in $\cot \theta$ (= pseudorapidity). Except for the end towers, this results in equal size scintillator pieces in a given layer. The first increment from 90° is 7.5° . The azimuthal sides of the module are closed by 1/4 in. steel cover plates. Directly inside of these is a 3/16 in. gap into which BBQ doped acrylic pieces are inserted, viewing the towers on their azimuthal faces. The 15° of azimuth subtended by a module corresponds to from 17 to 20 in. in scintillator width. A typical polar dimension is half that, for a typical scintillator size of 18 \times 9 in. Altogether there are 99 different sizes for the total 324 pieces in the module. Due to a shortage of scintillator, the 66 pieces for the third and fourth cells from the 90° end were replaced with inert material.

The inner cylindrical radius (distance from the proton/antiproton beam line) for the prototype is 66 in. and a one inch thick solid aluminum bottom plate occupies up to 67 in. A basic mechanical problem is to hold the stack on the aluminum plate, fastened onto the hadron calorimeter iron, in any azimuthal orientation, without allowing any pressure on the BBQ doped acrylic along the azimuthal boundaries. The mechanical connection to the hadron iron is made by a bolted rabbet joint of the end plates, and the shared 1/4 in. cover plates. The end plates and cover plates share the load of the shower counter variously according to azimuthal orientation. The shower counter stack is fixed by the lead mounting scheme and a pressure pad pushing against the innermost iron plate of the hadron calorimeter. The lead sheets are held at the end plates using centered ribs bolted on the inside of the end plates to match notches in a 5/8 in. tab at each end of each lead sheet. The tabs are reinforced by 1/8 in. steel riveted onto both sides. The lead sheets are

epoxy press clad on both sides with 0.015 in. aluminum which prevents lead creep when the lead, in a vertical plane, is held from the ends. The ribs also provide location during stacking.

We considered and tested both acrylic and polystyrene scintillator⁶. Light yield and attenuation length measurements confirmed previous reports⁷. We chose 0.236 inch thick KSTI390 polystyrene as the best match to our needs⁸. The light yield and uniformity in thickness of this extruded product outweighed the disadvantage of a relatively short attenuation length. Test measurements in which the scintillator was viewed with BBQ revealed an attenuation length in the scintillator of 17.3 in.

Individual scintillator pieces were saw cut slightly oversized and the two long edges were machined to give the desired longitudinal (θ) dimension, with the last pass using a diamond fly cutter. A small amount of buffing produced the clear optical surfaces required. In stacking, the scintillator pieces were wrapped by sheets of 0.002 in. vellum drawing paper above, below, and weaving. A test stack with paper wrapped scintillator showed no signs of surface wetting or other problems when placed under 20 psi for several days. The weight of the stack corresponds to about 2 psi, and the pressure pad will add a further 2 psi.

The proportional wire strip chambers were designed to be simply inserted in the stack on top of the third and ninth lead sheets. The basic wire channel and strip design is the same as the prototype used in laboratory tests³. The limited volume available for connections and the desire to have as much area active as possible are reflected in the details of design. A 3/4 in. gap was allotted for each chamber. The wires run lengthwise through the module so that the loss of active area at the azimuthal edges is only about 1/4 in. deep. This allows both for the chambers to be safely recessed while

the stack azimuthal face is being finished, and for electrical connections to be made to the strips which extend slightly beyond the aluminum. The cell size is 0.300 in. wide by 0.312 in. deep with 0.047 in. walls. Aluminum panels were gang milled in pieces 17 cells wide. Extrusions will be used for mass production. Three adjacent panels were glued to a 1/32 in. G10 sheet and trimmed to form a chamber. The inner chamber has 48 cells and the outer has 50. The strips for each chamber come on six separate 1/16 in. thick copper backed PC boards. The backs of these boards were made continuous ground. Slight cracks were left for source testing. The three boards toward the 90° end have 0.63 in. strip repeat distance and the other three have 0.75 in. spacing. The step reflects the wider effective spread of an electromagnetic shower as a function of angle of incidence. There are 137 strips on each chamber of the prototype. A multiple, rolled on layer of epoxy insulates the strips from the aluminum.

Figure 3 shows the end geometry of the chamber. The 0.002 in. gold coated tungsten wires are positioned nominally to ± 0.002 in. by machined rexolite standoffs which were a prototype for injection molding. Pairs of these standoffs are positioned close together at the middle of the chamber. This shortens the wire run length to about 46 in. and allows the wires to be cut at the center for separate readout at both ends, thus making each physical chamber two logical chambers. In fact, only eight consecutive wires on each chamber were split as a test. The wires were strung to 135 grams tension; the fastenings and the wire itself tested to yield at more than 400 grams tension. The wires are logically paired, and the readout and high voltage connections are made on 3/4 in. end PC boards mounted onto a shelf trimmed out of the aluminum. A sealed gas volume is formed by closing off with G10 strips so that all channels have gas flow in parallel. At the four corners, G10

pieces extend from the gas volume past the end of the lead and scintillator for connection to gas plumbing.

For economy, given the integrating nature of the readout electronics to be used,⁹ #30 twisted pair wirewrap wire was used for leads extending out to electronics on modules mounted on the back of the hadron calorimeter module (about 15 feet). The leads were soldered onto the end PC boards and strip boards. In order to guarantee strain relief and protection from the pressure in the stack, the leads are routed through and glued down in channels in a 1/8 in. thick layer of G10 glued to the back of the strip boards. This layer was covered by 1/32 in. G10 sheet, with the leads emerging at the four corners.

Various tests were made to assure performance. The high voltage standoff of the wires was checked in air before attaching the strip boards. Before placement in the stack, tests with ⁵⁵Fe x-rays at the exposed parts of the cracks between strip boards demonstrated viability and calibration of the chambers.

The overall shower counter stack was assembled on a set of five special clamps which, after the stack was complete, were adjusted to hold the stack together, at about 10 psi, rotated by 7.5° so that one face can be machined and finished. A second set of clamps was used to turn the stack to align the other face. A flycutter mounting disk was made so that the entire face could be flycut in one pass. Each face was completed in three passes, the last of which was a fine cleanup cut using a 3/8 in. radius diamond tool, as used in previously mentioned edging, set 0.002 in. deeper than an accompanying standard cutter. A small amount of buffing then yielded an acceptable optical surface.

Light collection occurs at the finished azimuthal faces which are viewed by pieces of 0.118 in. thick Rohaglas 2029¹⁰ BBQ doped acrylic. The average

separation between wavelength shifter pieces viewing adjacent towers is 3/4 in. Two schemes of guiding in the light past the hadron calorimeter to photomultipliers were tested. The fifth cell (from 90°) used a parallelogram shaped sheet of 0.118 in. thick Rohaglas 201¹¹ UVA acrylic extending beyond the iron to an adiabatic transition to an approximate circle. (The strips used to make adiabatic transitions were 0.118 in. thick Rohaglas 201.) In all other cells we used an adiabatic transition made from strips slightly less than 1 in. wide glued directly to each BBQ sheet, going to an approximately square cross section. A fairly abrupt turn to point outward is made with the individual strips in a bundle in order to keep the radius of curvature large compared to the plastic thickness. After the turn the bundle is glued to a 1 × 1 × 61 in. rod cut from UVA plexiglas sheet and machined and polished on all sides. The material and surface quality of the rods resulted in significantly poorer light transmission than commercially available rods. The first two towers employ simple, straight rods. The third and fourth towers are uninstrumented. The sixth through tenth cell rods are complicated by the nominal radial path to the back running into the 45° end of the module, and interference with similarly contorted hadron calorimeter lightguides. The ninth and tenth tower transitions are along the edge parallel to the end plate and start off in the 2 in. gap between the endplate and the lead and scintillator. Careful bending in three dimensions demonstrated the feasibility of solving the space problems of the shower counter and hadron calorimeter light guides.

We use Phillips XP2008 1 1/2 in. photomultipliers. The tubes selected for use had a width to peak ratio for BBQ spectrum quantum efficiency of ±10%. Each tube was glued onto a 1 3/8 in. diameter 1 1/2 in. long acrylic cookie which served as a mounting for a 0.056 in. Crofon¹¹ light fiber for connection

into a flasher system. The cookie was then glued to the end of a rod.

The BBQ material was measured to have an attenuation length of about 80 in. Ideally, to compensate for the different attenuation in the scintillator as the tower gets wider, the BBQ attenuation length should be 140 in. measured along a line perpendicular to the inner edge. To flatten the response, the inner BBQ edges were painted white.

Each completed, wrapped light guide assembly was then tested for its response to β 's passing directly through the BBQ. Some typical curves are shown in Figure 4. The results demonstrated the poor rod qualities, with the sheet assemblies significantly better than the rods, and straight rods better than curved rods. The response peak at the inside edge of the BBQ which results from the white paint, was compensated by inserting a mylar sheet, with light transmission of 80%, between the stack and the BBQ. The upper edge of the mylar is a sawtooth beginning 3/4 in. from the bottom (the inner edge) and ending 5 in. from the bottom.

Our initial tests in the M5 test beam at FNAL were carried out without the hadron calorimeter. The stack was banded together and rod light guides were supported by a frame. This run was used for detailed light yield measurements. Subsequently the shower counter was mounted to the hadron calorimeter iron which was held in a stand which allowed rotations and translation, equivalent to changing θ and ϕ about the interaction point. Appropriately shaped 1/8 in. aluminum spacer strips were inserted between BBQ pieces in order to ensure that the cover plate would not press on BBQ.

The important characteristics of the module are summarized in Table 1.

3. Beam Tests

The M5 test beam at FNAL provides tagged electrons and pions from 15 to

46 GeV/c. Remotely inserted lead stations before and after the first bend enhance and suppress the electron content of the beam respectively. Two threshold Cerenkov counters can separately veto electrons for pion selection; both were required for electron selection. The electron content of the tagged pion beam under similar circumstances has been reported to be of order 10^{-5} .¹² Our own data cannot rule out a contamination at the level of 3×10^{-4} or smaller. The tagged pions contained about 6% muons which could be separately selected.

Additional beam definition was provided by a set of counters a few feet upstream of the module. Two small trigger counters covered a 0.7 in. vertical by 0.5 in. horizontal hole between two large overlapping halo veto counters. One of the trigger counters was pulse height analyzed in order to help define single beam particles offline. The pion yield was generally enough to be tape speed limited by the MULTI¹³ system on the PDP 11/20, i.e. about 30 per spill. The electron trigger yield was considerably lower, in part because of the approximately 1 radiation length of material in the beam upstream of us. Electron triggers not incorporating the halo veto counters were completely dominated by multiple particles. Bremsstrahlung effects on fully selected electrons are evident in our results. A deadtime of at least 500 ns was generated for any beam particle and the trigger counter ADC gate continued for about 220 ns after the triggering pulse, to allow antiselection of triggers with late beam particles. In some cases the M5 yield was collimated to prevent distortions by rate effects.

Within the small defined beam spot (0.7 in. \times 0.5 in.), detailed information on the beam particle trajectory was provided by Directional Drift Chambers (DDC's)¹⁴ provided by M. Atac. The middle plane of three in each view is staggered to resolve the left-right ambiguity. This resolving reveals

a resolution of better than ± 0.008 in., which is more than adequate.

The local trigger counter signal, gated appropriately by upstream beam counters, deadtimes, busy signals, etc., set the timing for ADC gates and TDC starts for the DDC readout. The shower counter phototubes were read into LeCroy 2249A or 2249W ADC's, either directly or with up to 12 dB attenuation. High voltage settings were made according to quantum efficiency tests.

The same basic timing drove the LAC/WORM scanning integrating ADC system¹⁰ which was used to read out the strip chambers. The integrating times were 250 and 450 ns for wire and strip channels whose effective capacitances are about 400 and 900 pf, respectively, including leads.

4. Light yield

Adequate light yield is important both directly in energy resolution and indirectly in the ease of handling calibration and systematic effects. During our initial running we obtained samples of about 1000 electrons at each of four energies between 15 and 40 GeV and about 200 electrons at 10 GeV. The beam was centered in the first cell. The balanced sum of the two phototube pulseheights was demonstrated to be linear with electron energy to better than 1%. This sum for 40 GeV electrons is shown in Figure 5. The low energy tail is larger than would be expected¹⁵ from the known leakage. In fitting a Gaussian to these distributions, this tail was excluded from the fit, and the resulting variability of width is included in our systematic error. We believe that the considerable upstream radiator is the predominant source of the tail.

Results from our previous tests^{2,4} have agreed with the results of Stone et al.¹⁶ for sampling shower counters. The sampling fluctuations for our

counter, normal incidence, are expected to be $\pm 11.6\%/\sqrt{E}$ (GeV). Other contributions to observed resolution come from photostatistics and systematic effects. One large but easily understood systematic effect is the variation of pulse height across the beam spot introduced by attenuation in the scintillator. Data taken with electrons confirm the polystyrene sample measurement, and a fluctuation of slightly more than $\pm 1\%$ in each tube is produced. The fractional resolution due to both sampling and photostatistics should be proportional to $1/\sqrt{E}$. The fractional effects of the beam width, and perhaps other systematics, have other energy dependence.

To determine the light yield we unfold, as a function of $1/\sqrt{E}$; a.) the sampling and beam size effects from each tube, b.) the beam size effects from the ratio of the two pulse heights, in which sampling cancels, and c.) the sampling effects from sum of the pulse heights, in which the beam size effect is negligible. A consistent picture emerges of a light yield of 140 photoelectrons per GeV in the sum of both tubes. This result for the sum is shown in Figure 6. With generous allowance for systematic error, we quote our resolution as $(14.3 \pm 0.8\%)/\sqrt{E}$. The data of Figure 6 suggest but do not require the presence of a systematic term. We note that muon pulse heights correspond to about 250 MeV or about 35 photoelectrons in both tubes, which agrees with the calculations of Müller¹⁷.

Electron data were eventually obtained for all instrumented cells. Light yields for the different cells ranged from 70 to 190 photoelectrons per GeV. The variation from cell to cell followed the pattern of the light guide tests, e.g. the fifth cell, with sheet light guides, gave 190 p.e./GeV.

5. Uniformity

The attenuation of light in the scintillator gives rise to the largest

nonuniformity. Test beam and lab measurements, centered on the scintillator in the transverse dimension, agree on an attenuation length of about 17.3 in. The nominal width of the stack is 18.5 in. Thus the output of one PMT for a given ionization can vary by a factor of 3. There is a deviation from a pure exponential of about 6% in the form of excess at the extremes, near the azimuthal boundaries. This excess is cut off by shower leakage at the edge of the stack. Using the balanced sum of the tubes the variation is within a factor of 1.2. Systematic error, given position measurement, is negligible. If the pattern of energy deposited is sufficiently complicated in a given tower to preclude sorting out the geometry using the strip chambers, then one would expect systematic error in overall energy measurement, due to attenuation, within the factor of 1.2, i.e. about $\pm 6\%$, to be included with the presumably much larger hadron calorimeter measurement error.

The variation as a function of θ was measured by rotating the module about the nominal interaction point, moving the beam (30 GeV/c) from the first to the second cell. A slight dip at the boundary between cells is expected. The physical space between scintillators is about 0.020 in. Imperfect edge reflectivity of the scintillator and the gap between the BBQ/acrylic sheets viewing adjacent towers also give variation with θ . The effect of the gap is greater for showers near the azimuthal edges. This gap will be narrowed in the production design from about 3/4 to 3/8 in. The scan was taken with the beam aligned to the module corresponding to being 3.2° from the center in ϕ , that is, 4.3° away from the nearer ϕ boundary. The results are shown in Figure 7. The total variation is contained within a factor of 1.12.

To study the large effects of the crack between modules in azimuth, we rotated the module to put the bottom coverplate of the module into a horizontal plane and placed underneath a small shower counter and small hadron

calorimeter cells up against the surface. The entire assembly was then moved vertically to explore response near the crack. Although in detail the small modules have significantly different internal geometry than the prototype, the effects are roughly illustrated. The scan covered ± 4 in. from the the nominal boundary and used 1/2 in. steps in the region of rapid variation. We describe the results for 30 GeV electrons.

The shower counter retains its nominal response up to 1.5 in. from the boundary. At one inch there is an approximately 6% loss of response and a trace of response in the shower counter on the other side. We observed a gap region $1\frac{1}{4}$ in. wide, at the boundary. This region is characterized by response of the sum of the two shower counters averaging 15% of nominal. Averaged over azimuth, this gives a 6.4% loss in electromagnetic response. The total response, including the hadron calorimeter modules, gives a peak at the nominal energy of width about $\pm 8\%$ and a low tail which corresponds to 1% energy loss for photons averaged over azimuth. If the pulse height, which is mainly in the hadron calorimeter, is misinterpreted as being hadronic energy rather than electromagnetic, the position of the peak is systematically shifted, giving excess energy, 1.5% averaged over azimuth. Note that the geometry of the small hadron calorimeter modules is more favorable for recovering electromagnetic energy than another full scale module would be.

6. Wire chamber response to electrons

In M5 the two wire chambers were filled with 93/7 Ar/CO₂ gas. Operating voltages of 1490 and 1415 volts for the 2.5 and 6X₀ chambers, respectively, kept single channel pulse heights comfortably on scale. Extrapolation from tests made during construction suggest that the gas gain is about 10³ for the chamber located at 6X₀. The gain uniformity of the electronics channels¹⁰ was

previously demonstrated to be completely adequate¹⁸ and online monitoring only checked for malfunctions. The relatively large wire and strip dimensions, compared to the beam spot size, demanded careful attention to avoid artifacts of particular alignment. A square area of the two chambers consisting of all wire channels and a similar number of strip channels in the region of the beam was instrumented with electronics.

The Müller shower curves¹⁸ allow prediction of the mean pulse height response of a single sample, and our previous tests² have agreed reasonably well. The two chambers of this prototype reproduce previous results as shown in Figure 8. Chamber pulse height at $6X_0$ is nearly linear with energy. For 20 GeV and higher this represents by itself an energy measurement to better than $\pm 25\%$.

Considerable ability to sort out complex events is afforded by the correlation of the pulse heights of the wire and strip views. Tests of a prototype chamber with ^{55}Fe showed that in principle this correlation could be $\pm 5\%$ ³ neglecting both any pathological behavior of high energy electromagnetic showers and any nonuniformity across the area of the chambers. The correlations seen in the chambers for electrons, at a given location, are $\pm 14\%$ at $2.5X_0$ and $\pm 7\%$ at $6X_0$ showing the relative good behavior of 15 to 40 GeV electromagnetic showers near maximum. The points of the sweep data show a point to point variation in the correlation of $\pm 6\%$ suggesting that better tolerance uniformity or mapping of the correlation response of the $6X_0$ chambers is desirable.

We next address the question of how well optimized the widths of the strips and wire channels are at 0.63 and 0.69 in. respectively. The ability to distinguish nearby showers and the sharing required to give good interpolated position must be balanced against the cost of electronics

channels. The prototype design would require nearly 2×10^4 channels. The shower at $2.5X_0$ quite often tends to be very narrow, illuminating only one or two channels. The chamber design was optimized for shower maximum profiles, at $6X_0$, and performance of the $6X_0$ chamber will be detailed. Note that strip profiles are broadened by their induced nature.

Shower profiles are largely confined to three channels, with typically 93% of pulse height in the wire view and 87% in the strip view contained. This becomes 97% in both views for five channels. The two view correlation quoted as $\pm 7\%$ is valid for three channel pulse heights, and using either five or seven channels in both views gives only slight improvement. Thus the correlation is still useful for photons of comparable energy with two or more unoccupied channels between centers, 1.6 inches or more apart in both views. Note that the tail on the sides limits how near to one photon a photon of lower energy can remain visible.

The pulse height sharing in three channels is used to generate a coordinate. Because the beam size and strip size are comparable, we correlate the strip chamber coordinates to the DDC beam coordinates to isolate measurement effects. Unfortunately, this restricts us to a relatively small data sample in which all systems operated properly. The data are not sufficient to completely optimize coordinate algorithms. In the strip view a simple, linear, pulse height weighted average measures to ± 0.10 in. In the wire view a more complicated algorithm measures to ± 0.11 in. for the narrower profile and wider channels.

The linear algorithm gives ± 0.14 and ± 0.16 in. for the strip and wire views of the $2.5X_0$ chamber respectively. The narrow $2.5X_0$ shower profiles still do significantly better than would be obtained if the profiles were delta functions.

7. Electron identification

The combination of a momentum analyzed track and the shower counter and hadron calorimeter information provide considerable information useful in selecting an electron sample from a large hadron background. In this analysis we assume a solenoidal momentum resolution $\sigma_p/p = 0.002 \times p$ (GeV/c). In addition, 2 in. of aluminum was mounted upstream of the module to simulate the presence of the solenoid coil, corresponding to a then current design for a $0.6X_0$ thick coil¹⁹. Samples of about 2000 e^- triggers and 10000 π^- triggers at various energies and positions are used in this analysis.

To simulate the momentum resolution, each event is used 10 times with random Gaussian assigned momentum values. The assigned momentum determines the appropriate cuts on shower counter pulse height, hadron calorimeter pulse height, and both wire chamber pulse heights. Further cuts are made on the spatial width of pulse height distributions in the wire chambers. The effectiveness and correlation of these selections is illustrated in Table II, for 30 GeV e^- and π^- centered in the second tower. The overall result is a pion rejection factor for this run of $(7 \pm 2) \times 10^{-4}$ for 72% electron efficiency. Note that there is considerable correlation such that the cuts are much more effective alone than when applied after all others. Runs near normal incidence at 30, 40 and 46 GeV give similar rejections of $\lesssim 10^{-3}$ for 70% electron efficiency while runs at 15 and 20 GeV give $\sim 1.7 \times 10^{-3}$. At 40° incidence, 15 GeV gives 2×10^{-3} and 30 GeV gives 1.6×10^{-3} , all for 70% electron efficiency. The EM pulse height cut is adjusted to give the 70% electron acceptance.

For a large sample of 30 GeV data in the second tower the cuts were optimized for situations where some information is missing. Thus

$(0.7 \pm 0.2) \times 10^{-3}$ for all information becomes $(0.9 \pm 0.2) \times 10^{-3}$ with no $6X_0$ chamber, $(1.3 \pm 0.3) \times 10^{-3}$ with no $2.5X_0$ chamber and $(2.0 \pm 0.4) \times 10^{-3}$ for no chamber information. To simulate the case of running with no magnet, appropriate cuts were developed and for 70% electron acceptance the rejection is 1.5×10^{-3} for both chambers, 2.2×10^{-3} for the $6X_0$ chamber only and 2.7×10^{-3} for no chamber information. The fake electrons tend to have about 10% less measured energy than the parent pion energy. Background from pairs and Dalitz decays is neglected.

These results are an attempt to study the actual expected performance. If we increase the momentum smearing to $\sigma_p/p = 0.003 \times p$ instead of 0.002, the pion rejection degrades by about 40%. Our overall rejection is of the same order as the all neutral interaction rate for material upstream of the lead stack, and limited data we have support the idea that the rejection is proportional to the interaction lengths of material in front of the stack. Thus the rejection will degrade if the actual coil is thicker than we assumed. For the parameters of the CDF design report¹ a degradation of a factor of almost 2 may be expected from the above values.

8. Summary

We have demonstrated the feasibility of our design by constructing a full scale prototype. With a few modifications, the techniques seem quite appropriate for the construction of 50 modules. Detailed studies of calibration and monitoring systems are planned.

The shower counter module was demonstrated to yield sufficient light to give a resolution of better than $15\%/\sqrt{E}$ (GeV). The response map shows a variation in the two tube sum of 1.2 in the ϕ or attenuation length dimension and 1.1 in the θ or cell to cell direction. The chambers at 2.5 and $6X_0$ can

locate a 30 GeV shower to better than ± 0.16 and ± 0.11 in. respectively, as well as making a rough independent energy measurement and providing information to reject charged pions as electron candidates at a level of about 10^{-3} . The twenty-four fold azimuthal crack which contains wave shifters and light guides represents about a 6% inefficiency for observing electromagnetic energy in the shower counter. However, much of this energy may be recovered in the hadron calorimeter.

We are grateful to our various collaborators on CDF central calorimetry and to J. Urich, D. Hansen and C. Nelson for their help with the chamber electronics and to V. Frohne and the Meson staff for their cooperation. K. Coover and E. Walschon were of great help during construction. This work was supported by the U. S. Department of Energy.

Table I

Characteristics of the prototype module

Size: (1 of 48)	
Width	17-21 in. (15° of azimuth)
Length	98 in.
Active length	93 3/8 in.
Towers	10
Tower length	8-10 in., $\Delta\eta \sim 0.1$
Lead	32 \times 1/8 in., aluminum clad
Scintillator	33 \times 6 mm polystyrene (KSTI390)
Wave length shifter	0.118 in. acrylic (Rohaglas 2039)
Gap for shifter	0.188 in.
Light collection	
Primary	polystyrene
Secondary fluor	b-PBD
Recollection fluor	BBQ
PMT's	XP2008 (1 1/2 in.)
Chambers	
Cell size	0.312 \times 0.300 in.
Wire	0.002 in. gold coated tungsten
Wire logical width	0.69 in.
Strip widths	0.63 in., .75 in.
Depths (normal)	2.5 X_0 , 6 X_0

Table II
Electron Selection Criteria

Cut	electron survival	pion survival	remaining pion survival after all other cuts
EM Scintillator	0.87	0.0076	0.29
Hadron Calorimeter	0.94	0.013	0.54
W1 Pulse Height ($25X_0$)	0.94	0.24	0.54
W2 Pulse Height ($6X_0$)	0.97	0.041	0.90
W1 Width	0.99	0.24	0.89
W2 Width	0.97	0.23	0.69
TOTAL	0.72	7×10^{-4}	

References

1. D. Ayres et al., Design Report for the Fermilab Collider Detector Facility, Fermilab internal note CDF-t11 (1981) (unpublished).
2. M. Atac et al., CDF-27 (1978) (unpublished).
3. L. Nodulman, Nucl. Instr. and Meth. 176 (1980) 345.
4. D. S. Ayres, et al., CDF-50 (1980) (unpublished).
5. End plates with keyways were provided by the Purdue High Energy Physics group.
6. B. Kustom et al., CDF-67 (1980) (unpublished).
7. M. Bourdinard, J. C. Thevenin, Physica Scripta 23 (1981) 534.
8. Scintillator was made by KSH Inc. in Belgium with quality control by the Saclay group.
9. T. F. Droege et al., IEEE NS27 (1979) 64.
10. Wavelength shifters were obtained from Rohm GMBH, Darmstadt.
11. Commercial plastic light fibers developed by DuPont.
12. Y. Sakai et al., IEEE NS28 (1981) 528.
13. L. M. Taff et al., FNAL PN-974 (1978) (unpublished).
14. M. Atac et al., IEEE NS25 (1978) 30.
15. B. Musgrave, CDF-23 (1978) (unpublished).
16. S. L. Stone et al., Nucl. Instr. and Meth. 151 (1978) 387.
17. D. Müeller, Phys. Rev. 5 (1972) 2677.
18. M. Atac et al., IEEE N528 (1981) 500.
19. D. Cline et al., FNAL TM-826 (1978) (unpublished).
20. T. Kamon et al. (in preparation); Kyowa Gas Chemical Industry Co., Niigata Japan.

APPENDIX

Design Changes for Production

Several design changes have been made for production modules. The inner radius has been moved out from 66 to 68 inches in order to allow for some future added detector. The steel cover plates change from 1/4 to 3/16 inch thick and the gaps between the cover plates and the stacks which contains the WLS sheets increases from 3/16 to 1/4 inch to allow greater tolerance. As discussed above, the gaps between WLS sheets will be reduced to 3/16 inch. Commercial rods will be used as lightguides. To avoid an awkward glue joint, the transition strips will be laser cut into WLS material.

Only one strip chamber will be used, at 6 X_0 . The cell size has been decreased to 0.25 inches and the aluminum panels are extruded. Improved injection molded wire standoffs will facilitate splitting the wires. The strip widths have been slightly increased to give 128 strip channels per chamber along with 32 wire channels per end. The strip boards have plated-through holes to simplify the connecting of leads. Given the extreme difficulty of getting at the chamber for repair, each logical wire channel will have its own high voltage lead which can be disconnected outside the module.

An improved scintillator and WLS combination has been developed in Japan.²⁰ Cast polystyrene scintillator containing a secondary, UV to blue fluor is coupled to a new blue to green WLS. Despite changing the scintillator thickness from 0.24 to 0.20 inches, both the light yield and the scintillator attenuation length will be significantly increased.

The coil design now shows approximately one radiation length of mostly aluminum in front of the central shower counter, for normal incidence. Because of this increase of material, and to help slightly in hadron rejection, the stack has been reduced from 32 to 30 lead layers. By partially replacing lead with acrylic in several layers, both the wire chamber depth and the overall thickness, in radiation lengths, are kept nearly constant as functions of polar angle. The average thickness will be $19.4 X_0$, which is nearly identical to the prototype module without a mock coil, which produced the data shown in Figure 5.

Figure Captions

1. Layout of the central detectors proposed for the FNAL Collider Detector Facility. a) Overall view with one side rolled out. b) Quartersection.
2. Layout of the electromagnetic calorimeters of one of 48 central modules. A hypothetical all rod lightguide design is shown.
3. End geometry of the channel strip chambers.
4. Typical response curves for BBQ and light guide assemblies to straight through betas. The coordinate is cylindrical radius with zero taken at the inner, white painted edge of the wavelength shifter. T and B refer to top and bottom in the test beam orientation.
5. Typical phototube response: 40 GeV electrons in the first (90°) cell.
6. Resolution as a function of electron energy.
7. Pulse height variation in a polar angle scan. Zero is set to the first cell center. The second cell center is at about 7 degrees.
8. Pulse height linearity (A) and resolution (B) of the two wire strip chambers for normal (N) and diagonal (D) incidence ($\sim 40^\circ$). Previous results for resolution of a single sample extend to lower energies.

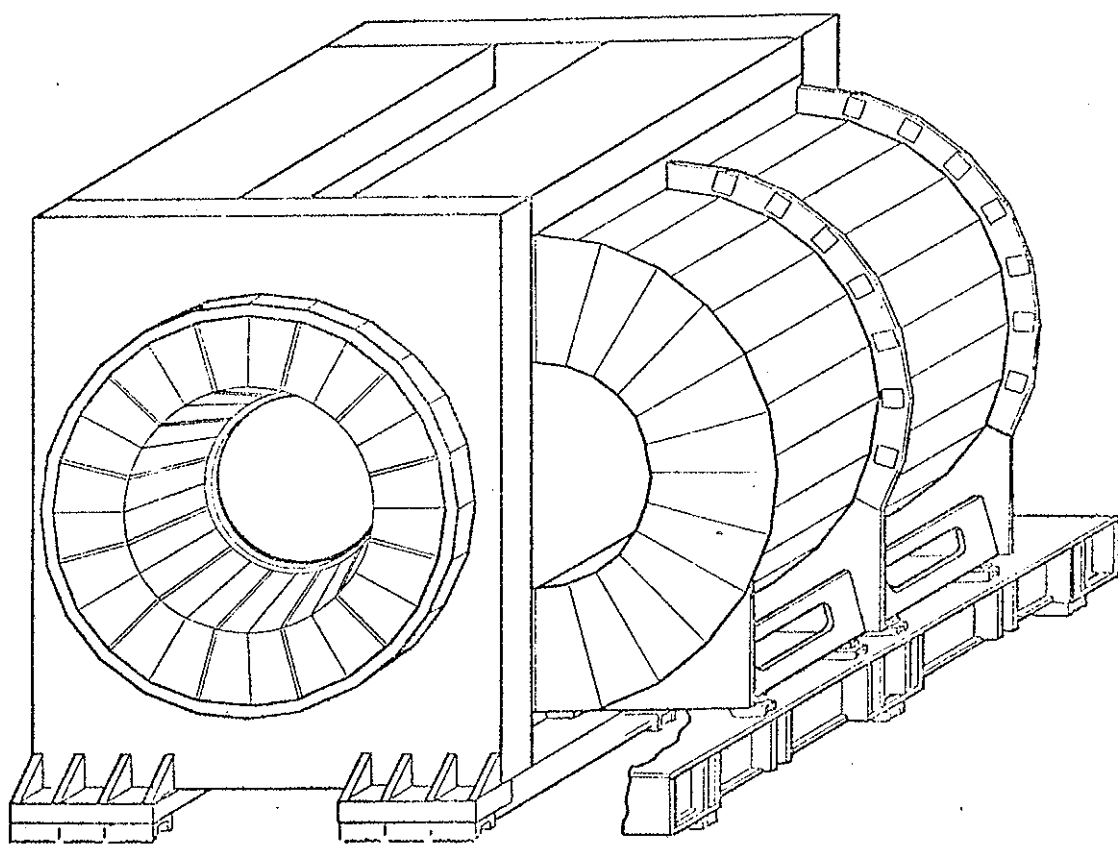


Figure 1a

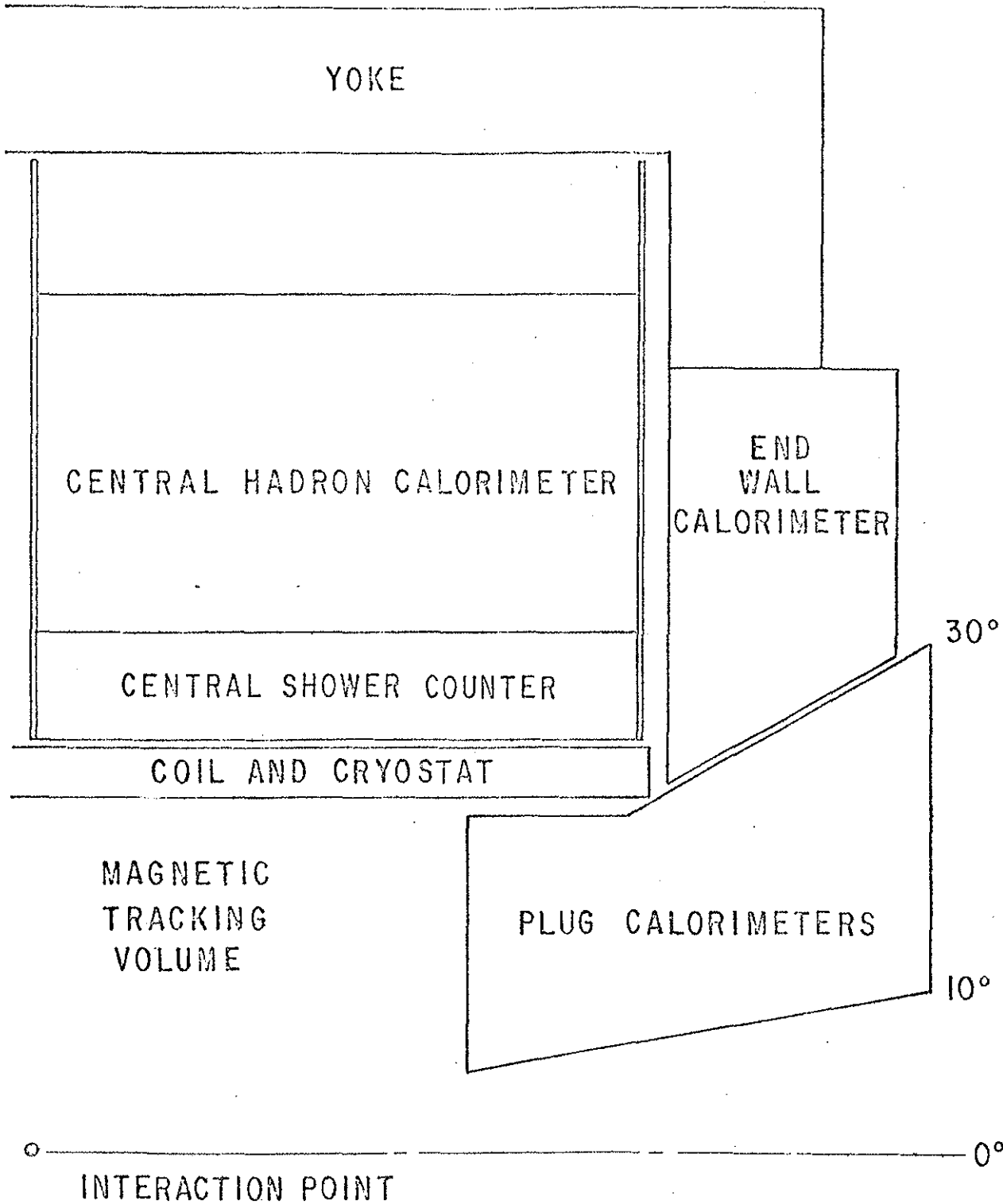


Figure 1b

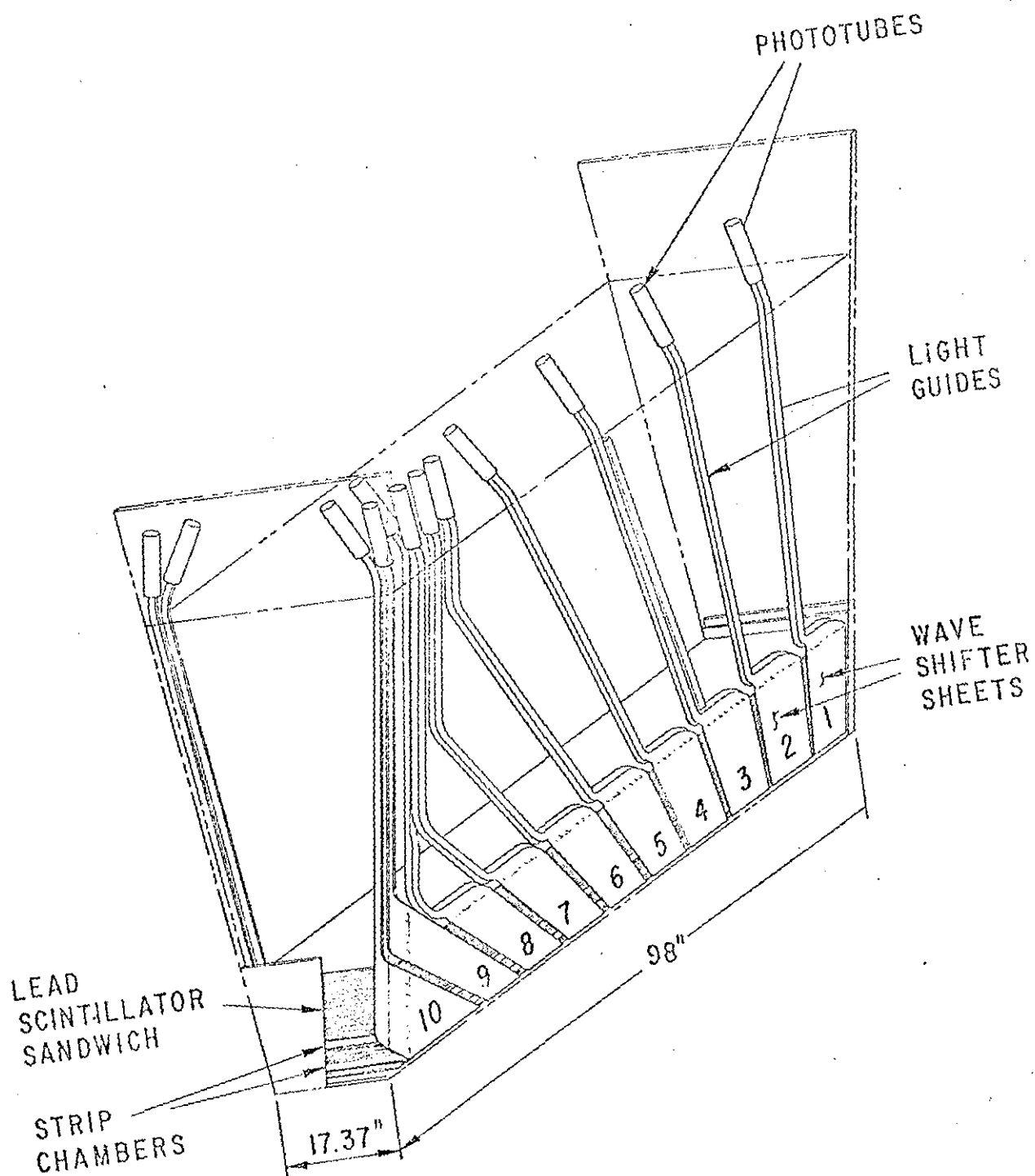


Figure 2

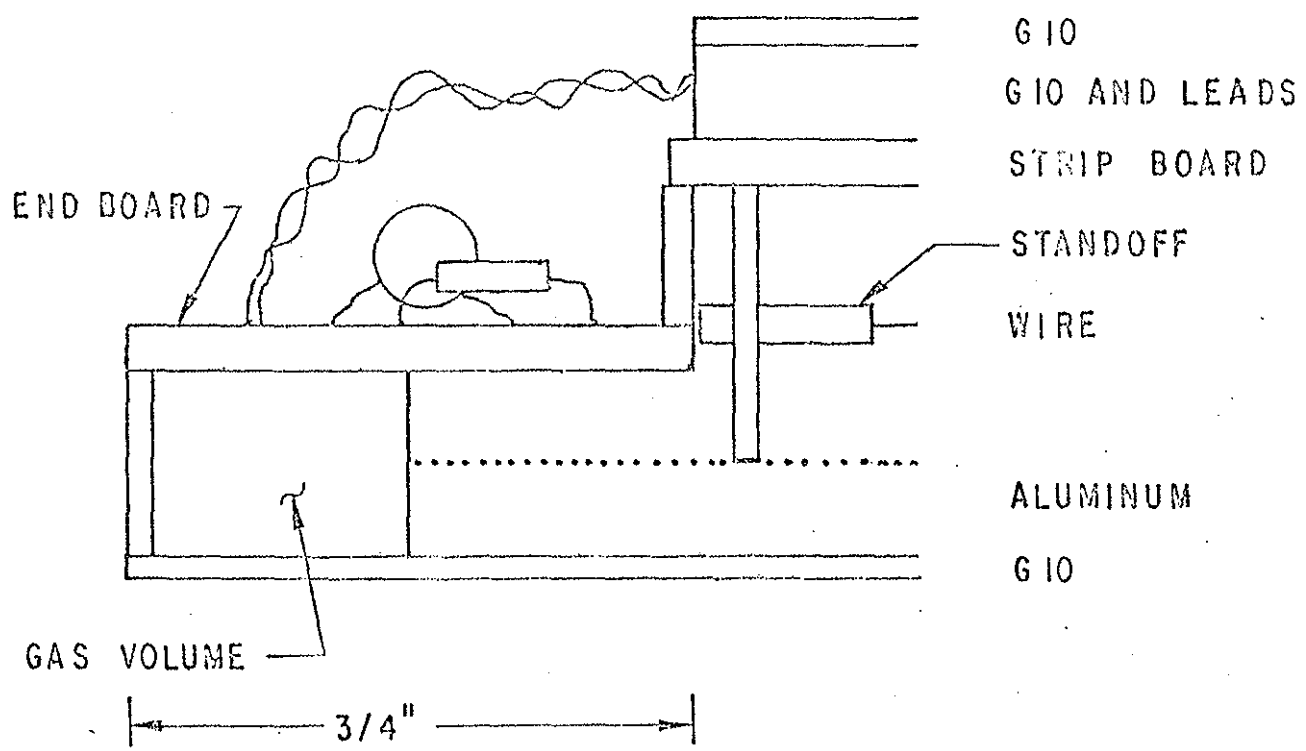


Figure 3

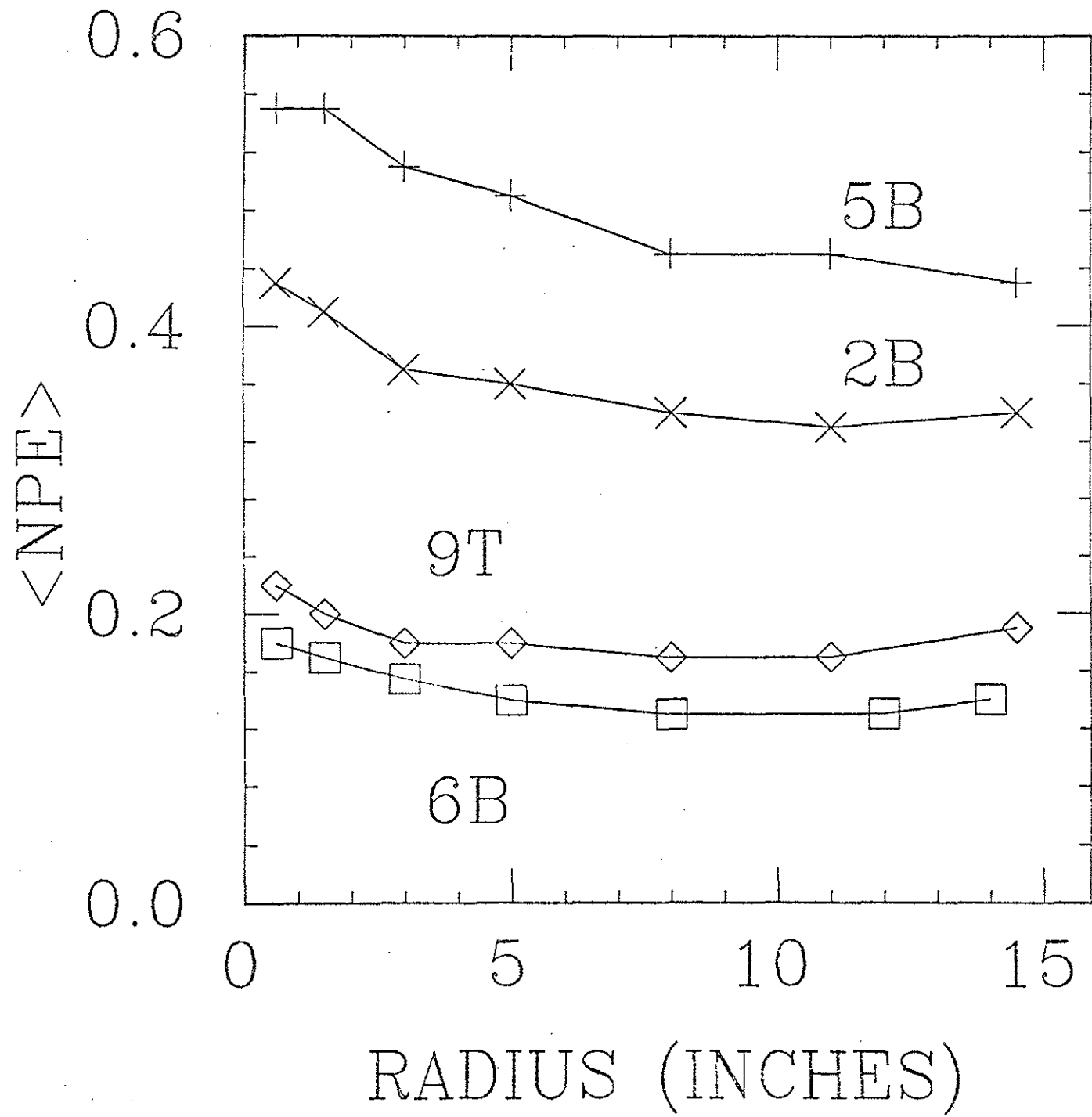


Figure 4

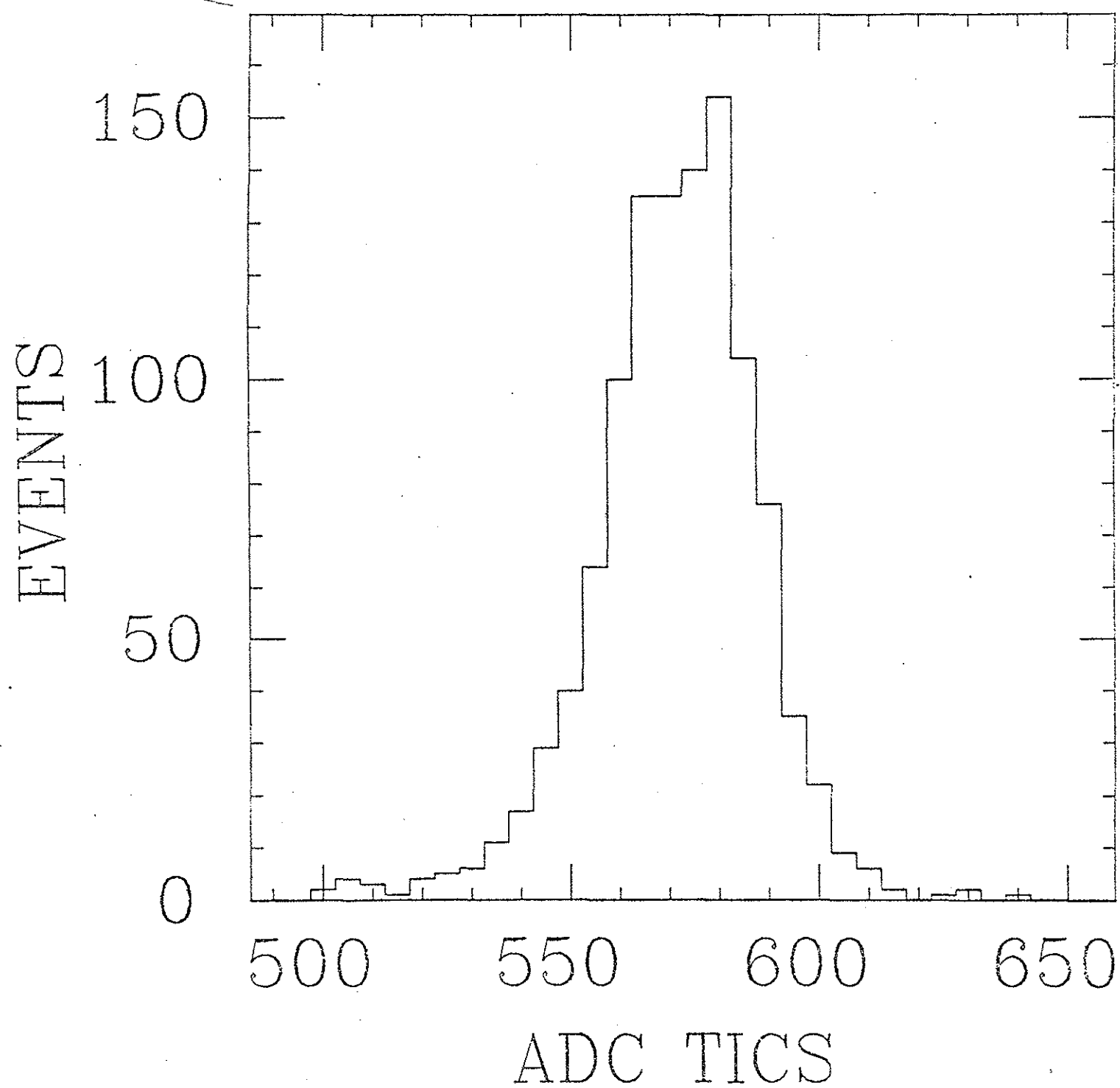


Figure 5

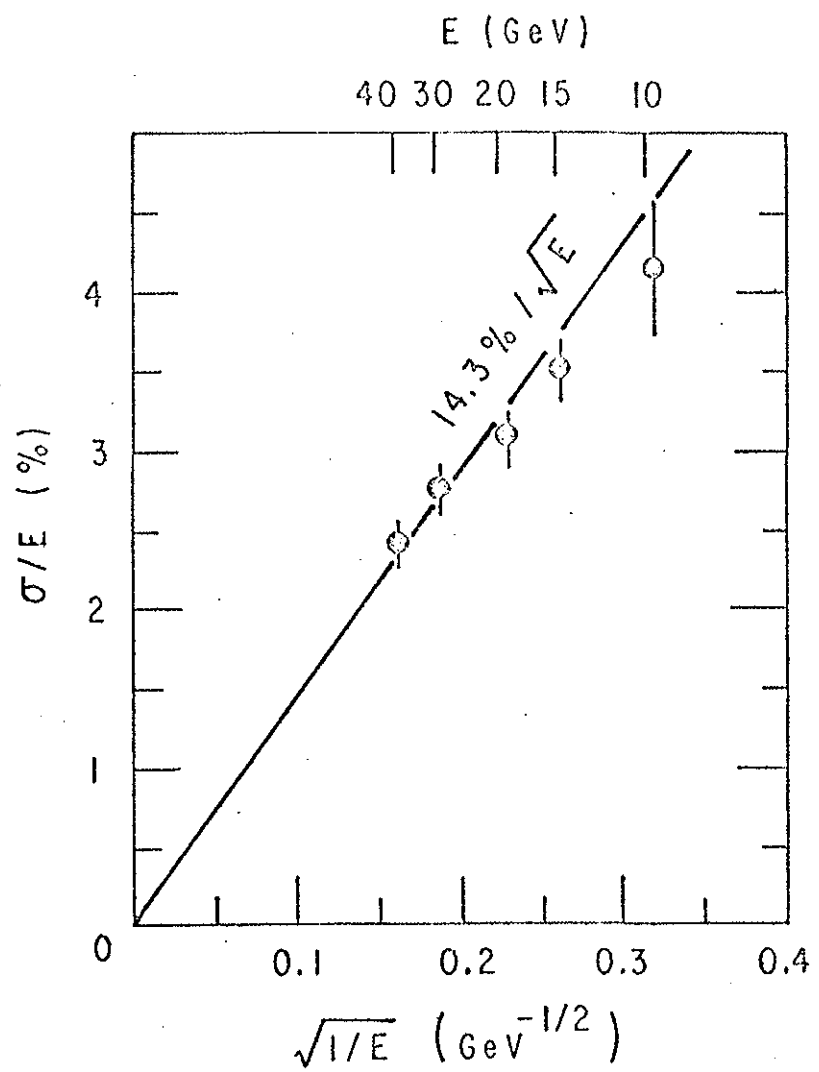


Figure 6

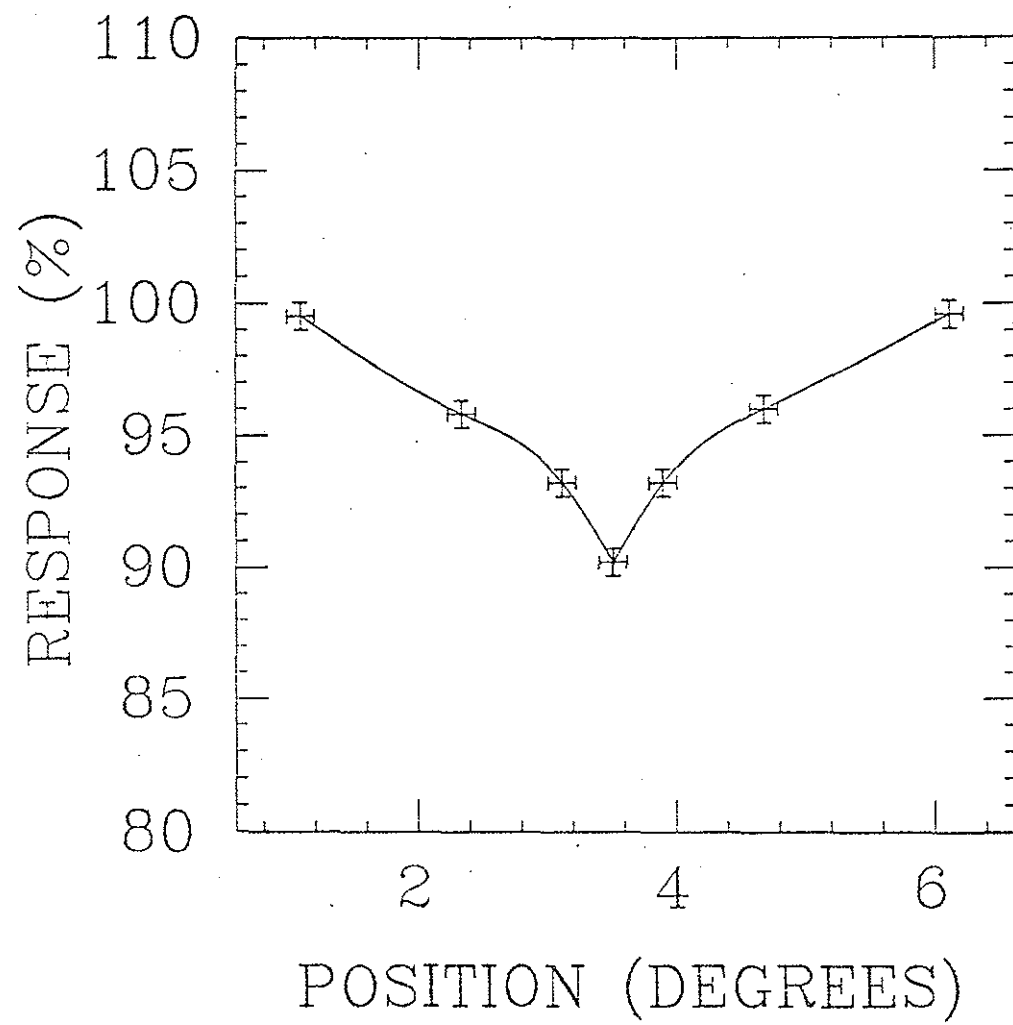


Figure 7

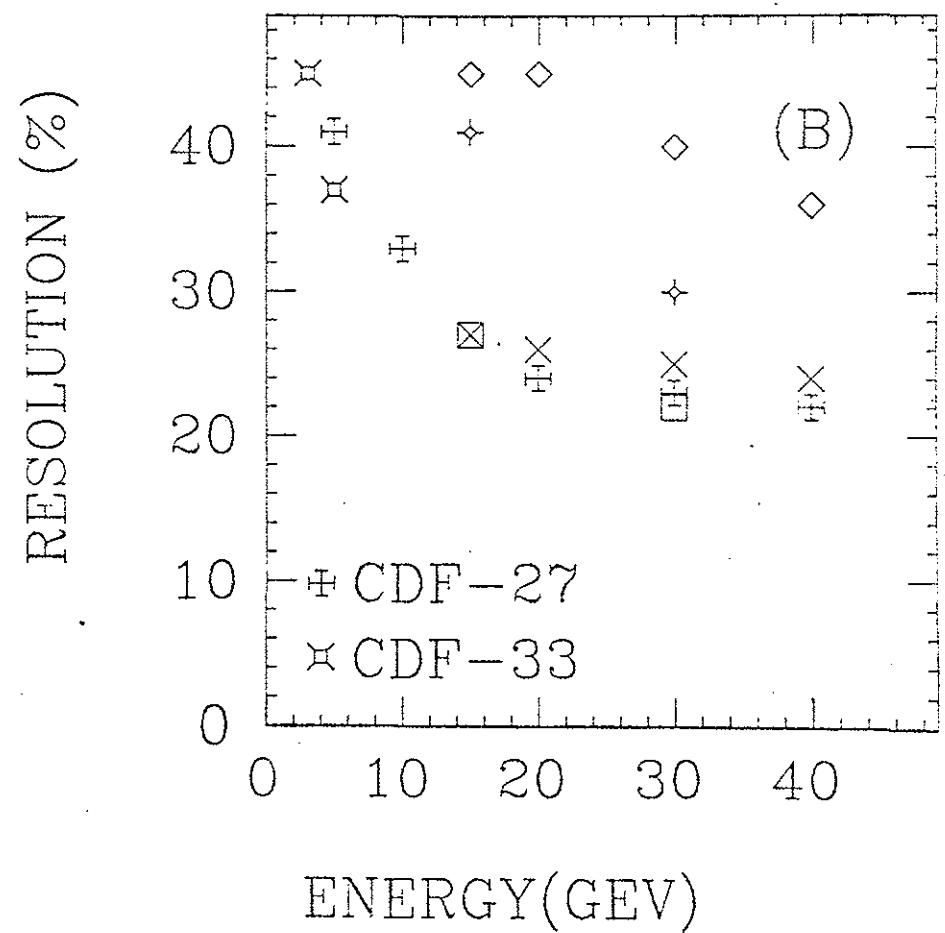
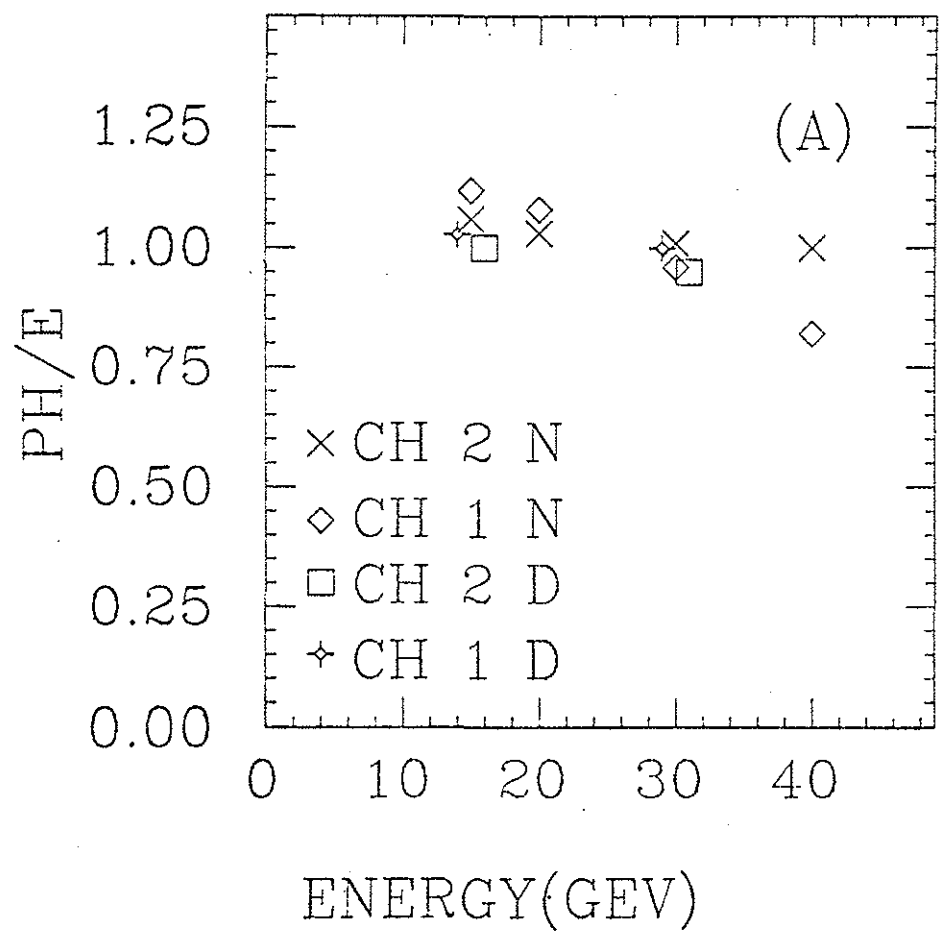


Figure 8